

# Redox Processes of Methyl Viologen Cation Radicals at Zeolite Y-Modified Electrodes

Tit-Wah Hui and Mark D. Baker\*

Department of Chemistry and Biochemistry, Guelph-Waterloo Centre for Graduate Work in Chemistry, Electrochemical Technology Centre, University of Guelph, Guelph, Ontario, Canada N1G 2W1

Received: August 7, 2001; In Final Form: November 10, 2001

Enhanced currents observed for reduction of methyl viologen cation radicals at zeolite Y-modified electrodes are due to comproportionation reactions. These occur between methyl viologen dications and zerovalent methyl viologen ( $MV^0$ ) deposited on the electrode surface. Double potential step chronocoulometry (DPSC) confirms that the presence of adsorbed  $MV^0$  on the conductive portion of the electrode. Moreover, in the presence of a surfactant, DPSC shows that the adsorbed phase dissolves with a reduction in the significance of comproportionation. Electron transport is unequivocally occurring outside the zeolite network because of the size and charge rejection of the anionic surfactant. Electrolyte cation-induced changes in the modified-electrode response are discussed in terms of ion exchange rates, and deposition–dissolution effects.

## Introduction

Electrochemical reduction of methyl viologen dications ( $MV^{2+}$ ) to cation radicals ( $MV^{+•}$ ) at zeolite Y-modified electrodes occurs via an extrazeolite redox process rate limited by ion exchange kinetics.<sup>1</sup> Reduction of  $MV^{+•}$  however, produces complex electrochemistry that has been difficult to interpret.<sup>2–5</sup> Interestingly, the cyclic voltammetry observed in the presence of the zeolite is considerably different from that observed in the solution phase. In the former case, significant comproportionation between the dication and the neutral methyl viologen molecule (eq 1) can occur.



Since this process re-forms the reactant radical, the current for the  $MV^{+•}/MV^0$  cathodic peak is enhanced as the potential is scanned through the second reduction process. Calzaferri and co-workers<sup>5</sup> reported cyclic voltammetry of “monograin” zeolite-modified electrodes containing the methyl viologen dication. Current enhancement in the second reduction wave occurred in both LiCl and NaCl electrolytes. This was interpreted in terms of intrazeolite comproportionation, necessitating that the methyl viologen cation radical was constrained within the zeolite. An interesting dependence on the nature of the electrolyte cation was observed, showing a decrease in the reduction peak current for  $MV^{+•/0}$ , in the order  $Li^+ > Na^+ > K^+ > Cs^+$ . Ion exchange kinetics for supercage moieties such as methyl viologen proceed via the solvated alkali cations and so, based on the solvated ionic radii, it is expected that leaching of  $MV^{2+}$  into solution will accelerate as the alkali metal group is descended. As a consequence intrazeolite electron transfer will lessen in importance, in apparent agreement with this observation.

Intrazeolite comproportionation followed by further reduction within the zeolite pore system must follow reduction of  $MV^{2+}$  at the outer region of the zeolite, which is coupled to a slow loss of surface  $MV^{2+}$  and  $MV^{+•}$  into the electrolyte solution.<sup>1</sup>  $MV^{+•}$  formed at the surface supercages once reduced to  $MV^0$  would then react with adjacent  $MV^{2+}$ . Further reduction of bulk  $MV^{2+}$  must then occur via electron hopping between  $MV^0$  and  $MV^{+•}$ . Since comproportionation and electron hopping between

$MV^0$  and  $MV^{+•}$  are required to occur simultaneously, their rates should be comparable to that of physical movement of  $MV^0$ . Loss of  $MV^0$  from the zeolite will retard this charge propagation process. In the remainder of this paper we discuss the manner in which redox occurs in this system. Emphasis will be placed on chronocoulometric measurements.

## Experimental Section

NaY was from Union Carbide (LZY-52). Methyl viologen (*N,N'*-dimethyl-4,4'-bipyridyl dichloride) was purchased from Aldrich and used without further purification. All electrolytes (Aldrich) were reagent grade and were used as received. Water used in all experiments was from a Barnstead water purification system. The final resistivity was 18 MΩ cm. Polystyrene (MW = 32 600, Aldrich) was used as received. Prior to ion exchange, zeolites were stirred in 1 M NaCl for 24 h to remove impurity cations and/or protons and were then filtered and washed. Different loadings of methyl viologen-exchanged zeolite Y samples were prepared by ion exchanging a stoichiometric amount of methyl viologen into NaY. A 1 g sample of NaY was stirred in 250 mL of water containing methyl viologen dichloride for 24 h. The zeolite was then air-dried and stored for future use. Loadings of methyl viologen were determined by dissolution of the zeolite in 2 M HCl followed by UV spectrophotometry. A value of  $2 \times 10^4 \text{ M}^{-1} \text{ cm}^{-1}$  at  $\lambda_{\text{max}}$  258 nm was used<sup>5</sup> for the absorption coefficient. Loadings of  $MV^{2+}$  are reported as the percentage of  $Na^+$  ions exchanged. Crystallinity of the zeolites was assessed with XRD, showing no measurable loss in lattice integrity.

Monograin layer ZMEs were prepared using a modification of literature methods.<sup>5</sup> Teflon-sheathed glassy carbon rods (3 mm diameter) were polished with 0.05 μm alumina, ultrasonically washed and then air-dried. A 5 mg sample of the zeolite was then dispersed in 3 mL of water and stirred vigorously for 30 min. A 3 μL aliquot of the dispersion was then applied onto the polished glassy carbon surface and air-dried. Onto the dried zeolite layer was added 1 μL of a 0.75 mg polystyrene in 20 mL of tetrahydrofuran solution and it was allowed to evaporate. The final coating contained 5 μg of zeolite and 0.04 μg of polystyrene. Electrochemical data were recorded using an

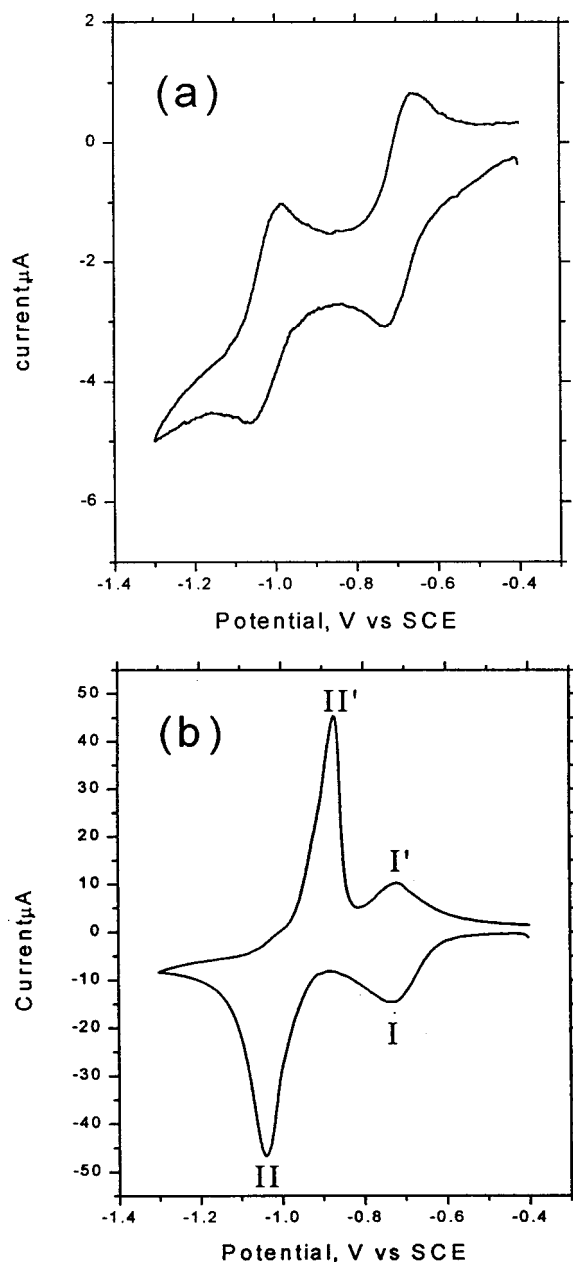


**Figure 1.** Cyclic voltammetry of (a) 0.3 mM  $\text{MVCl}_2$  and (b) 58% MVY in 0.05 M LiCl. Scan rate: 20 mV/s.

EG&G 273A potentiostat. A two-compartment, three electrode cell was used in all experiments. The counter electrode was a 1  $\text{cm}^2$  platinum flag, and the reference electrode was a saturated calomel electrode (SCE). The working and counter electrode were placed in the working compartment with the SCE in a separate compartment. Prior to data collection the electrolyte solution was purged with oxygen free nitrogen for 20 min. All experiments were run without IR compensation. Cyclic voltammograms were recorded immediately following immersion of the electrodes. Chronocoulometry was recorded in a similar fashion. Step potentials are given in the body of the paper. All potentials are with respect to SCE. Surfactants were obtained from Aldrich and were used as received.

## Results and Discussion

**Cyclic Voltammetry.** Cyclic voltammetry of methyl viologen Y zeolite-modified electrodes (MVY) is shown in Figure 1. In agreement with the work of Calzaferri et al.<sup>5</sup> significant current

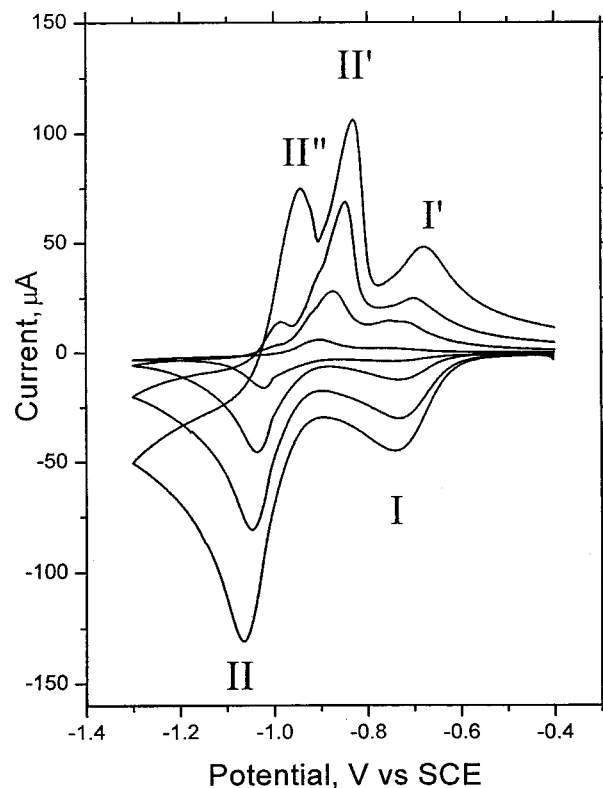


**Figure 2.** Cyclic voltammetry of 58% MVY in 0.1 M LiCl. Scan rates from top to bottom: 100, 50, 20, 5 mV/s.

enhancement in the second cathodic wave is apparent. Voltammetry at a bare glassy carbon electrode is also displayed for comparison purposes. It is inappropriate to interpret these data solely in terms of promoted comproportionation as we now discuss. Equation 1 indicates that  $\text{MV}^\circ$  is involved in comproportionation, and so a diminished reoxidation wave (peak II':  $\text{MV}^\circ \rightarrow \text{MV}^{+\bullet}$ ), should result. Similarly, an enhanced peak I' ( $\text{MV}^{+\bullet} \rightarrow \text{MV}^{2+}$ ) is expected due to the accumulation of  $\text{MV}^{+\bullet}$  (i.e., a normal EC' response). MVY electrodes do not exhibit a normal EC' response, where a nondiminished peak II' is obtained.

Figure 2 shows cyclic voltammograms of 58% MVY at various scan rates. Increasing the scan rate gives rise to a new (anodic) peak II'' at about  $-0.95$  V. Similar results have been reported by Engelman and Evans,<sup>6</sup> and Feng et al.<sup>7</sup> in aqueous media. They concluded that peak II'' was due to oxidation of amorphously deposited  $\text{MV}^\circ$ , and that peak II' indicated a more stable crystalline deposit. At slower scan rates the amorphous deposit converted into the crystalline phase. Figure 3 shows the cyclic voltammetry of MVY at various loadings and scan rates. The growth of an anodic peak at about  $-0.95$  V with increasing scan rate apparently reflects deposition of  $\text{MV}^\circ$  on the glassy carbon substrate. This is observed at all loadings. Deposition appears to occur on the conductive electrode surface, since  $\text{MV}^\circ$  will adsorb on hydrophobic glassy carbon rather than on the hydrophilic zeolite. Conproportionation between  $\text{MV}^\circ$  and  $\text{MV}^{2+}$ , therefore, likely occurs at the electrode surface, and not in the bulk of the zeolite particles. Note that the smaller currents in the reverse scan are due to loss of viologen from the electroactive zone.<sup>1</sup> These notions are upheld by double-potential-step-chronocoulometry (DPSC), which we now discuss.

**Chronocoulometry.** In DPSC the  $x$ -axis is displayed as  $t^{1/2}$  or  $\theta^{1/2}$  for the forward and reverse steps, respectively. In the reverse step  $\theta^{1/2}$  is given by  $(\tau^{1/2} + (t - \tau^{1/2}) - t^{1/2})$ , where  $t$  is

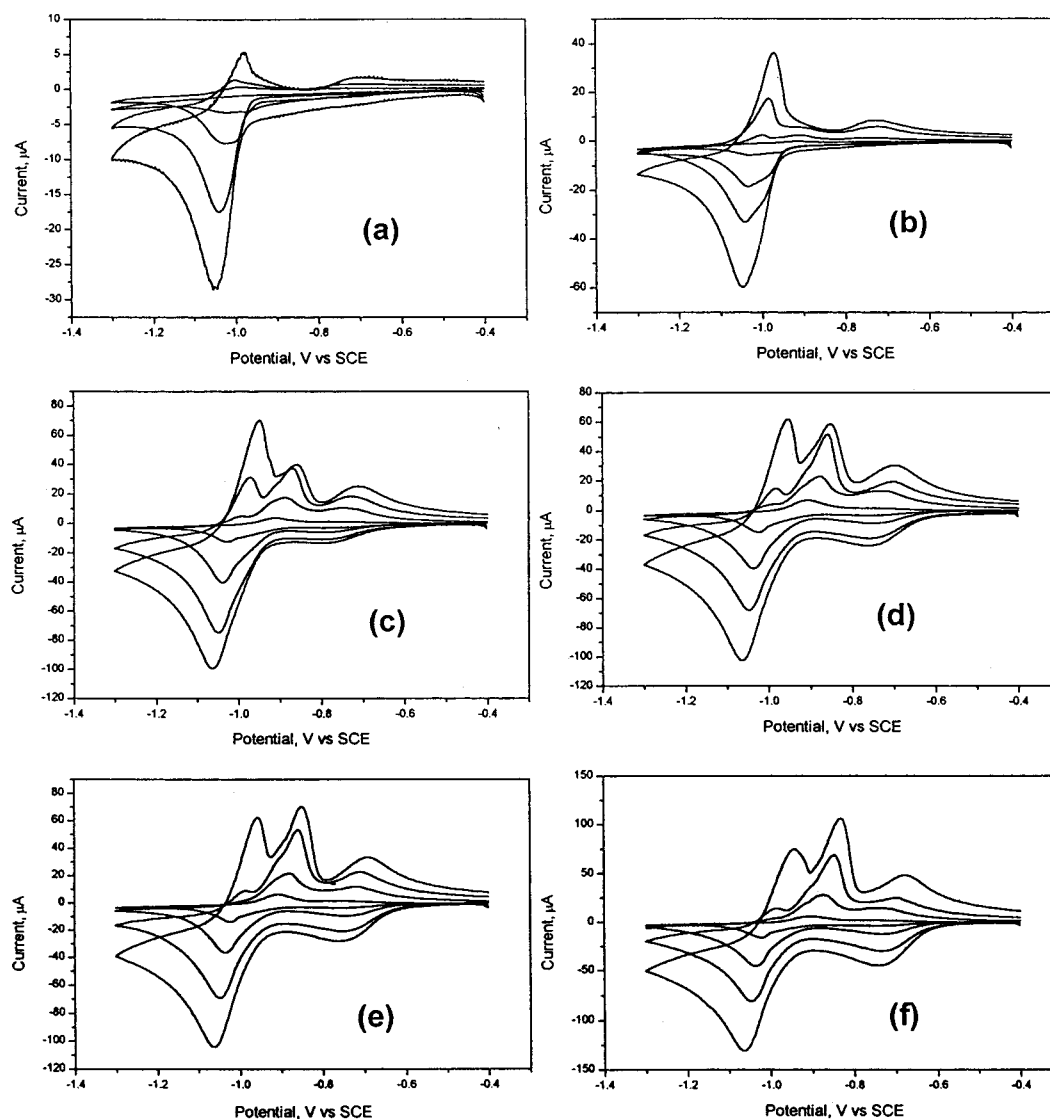


**Figure 3.** Cyclic voltammograms of (a) 3.2%, (b) 8.3%, (c) 25%, (d) 37%, (e) 42%, and (f) 58% MVY in 0.05 M LiCl. Scan rates from bottom to top: 100, 50, 20, and 5 mV/s.

the duration time of the potential step and  $\tau$  is the switching time. In this paper the upper plot is for the forward (reductive step) and is thus plotted against  $t^{1/2}$ . In the upper plot, the y-axis is the total charge passed in the reductive step,  $Q_r$ , and in the lower plot  $Q_r$ , the charge for reoxidation in the reverse step, is used.  $Q_r$  is given by  $Q_r - Q_i$ , where  $Q_i$  is the charge passed at the switching time. In the discussion below, the electroactive fraction is determined by dividing the number of moles participating in the redox reaction by the total number of moles of viologen initially present in the zeolite.

DPSC of viologens in water (and in the absence of a zeolite phase) show<sup>8-10</sup> a diffusion-controlled forward (reductive) step giving linear  $Q$  vs  $t^{1/2}$  plots passing through the origin in agreement with the Cottrell equation. The reverse step plots, however, often show a sharp increase in charge followed by an abrupt change to a straight line with a smaller slope (also see Figure 4 described below). This is typical for deposition of the reduction products from the forward step.<sup>11,12</sup> Finite-difference digital simulations by Engelman and co-workers<sup>9</sup> show that extrapolation of the linear region gives a negative intercept of charge, the magnitude of which is equivalent to the total amount of neutral deposits. The duration of the slope change occurring in the reverse step is dependent on the deposition rate constant,

diffusion coefficient of the neutral species, and the switching time.

DPSC for 8.3% exchanged MVY is shown in Figure 4. During the reductive step the data deviate from Cottrellian behavior at longer times since  $MV^{2+}$  is depleted from the electroactive zone, as viologens exit the zeolite into the solution phase. At about  $\theta^{1/2} = 0.2$ , a sharp change in slope in the reverse step occurs. This is indicative of adsorption and is in accord with the voltammetry described above. Extrapolation gives an intercept of 28.7 mC, which is 22% of the total electroactive fraction, while the total charge passed in the forward step was 42% of the electroactive fraction. The data for MVY at different loadings are tabulated in Table 1. At lower loadings the fraction for both the forward and deposition processes increase. This suggests that electron hopping is not occurring since the probability for an electron to hop between the viologen moieties decreases with diminished concentration of the redox centers. This would result in a decrease in the electroactive fraction. At all lower loadings, about half of the  $MV^\circ$  produced from the forward step deposits on the electrode. The remaining  $MV^\circ$  may diffuse into the bulk solution, rather than into the hydrophilic zeolite; however, as we now show, the remaining charge that flows in the forward step is actually due to the reduction of

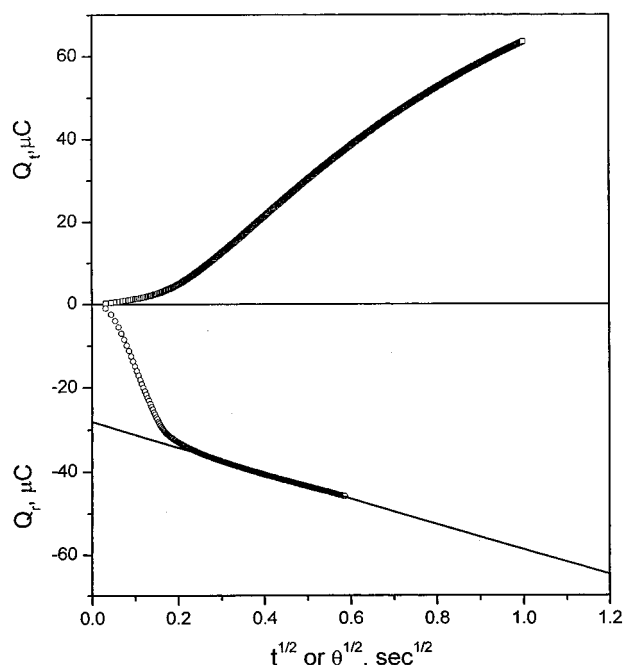


**Figure 4.** DPSC plots for 8.3% MVY in 0.05 M LiCl. Potential step from  $-0.4$  to  $-1.3$  V for 1 s.

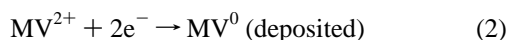
**TABLE 1: Electroactive Fractions Obtained from DPSC of 5  $\mu$ g of MVY on Glassy Carbon Electrodes in 0.05 M LiCl (Potential Step from  $-0.4$  to  $-1.3$  V for 1 s)**

loading, %	electroactive fraction		percentage deposition, <sup>c</sup> %
	total, <sup>a</sup> %	deposition, <sup>b</sup> %	
3.2	44	24	54
8.3	42	22	52
25	36	16	44
37	24	12	50
42	24	11	46
58	24	9	38

<sup>a</sup> Calculated from the total charge at switching time. <sup>b</sup> Calculated from the y-intercept of  $Q_r$  vs  $\theta^{1/2}$  plots. <sup>c</sup> Calculated by dividing the electroactive fraction for deposition by the total electroactive fraction.

$MV^{2+}$  to  $MV^{+\bullet}$  rather than the formation of  $MV^\circ$  that is not deposited on the electrode surface.

**Deposition and Dissolution.** Consider the case where the electrode potential is stepped cathodically so that the following reaction occurs.



When deposition starts, the free electrode area,  $A_f$ , available for electrochemical reduction decreases and the area of the deposit,  $A_d$ , increases. Conproportionation dissolves the deposit (see eq 1), the rate increasing as  $A_d$  increases. If the electrode is not totally covered with deposits,  $MV^{+\bullet}$  can reduce to  $MV^\circ$ . The equilibrium constant for conproportionation of the solution species based on the reversible potentials for the two reduction steps, is of the order of  $10^7$ . If conproportionation is rapid, a steady state can be achieved where the rate of formation of the deposit equals the rate of dissolution. Then the net process is merely the reduction of the dication to the cation radical being the sum of eqs 1 and 2, i.e.,



Most of the charge is then passed in the reduction of  $MV^{2+}$  to  $MV^{+\bullet}$  and net deposition will occur only if the electrode is not

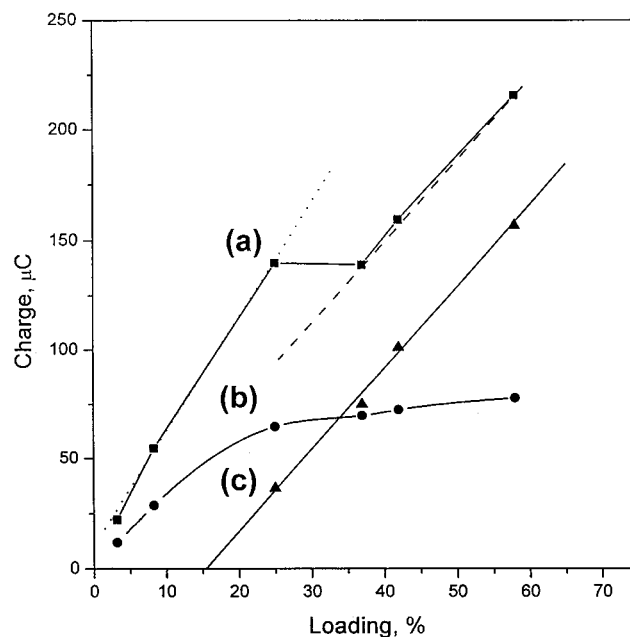


**Figure 5.** Charge versus loading plots. (a) Total charge recorded at the switching time ( $\tau = 1$  s) in DPSC (potential step  $-0.4$  to  $-1.3$  V). (b) Charge for the deposits obtained by the y-intercept in  $Q_r$  vs  $\theta^{1/2}$  plots. (c) Calculated by multiplying by a factor of 2 by the charge at the switching time. Potential step:  $-0.4$  to  $-0.9$  V.

saturated. We now discuss deposition–dissolution for MVY using DPSC.

Figure 5 shows DPSC data for various loadings of MVY. Curve a shows the total charge passed at the switching time, which corresponds to the total charge required for the deposition and conproportionation reactions (i.e., eqs 1–3). Curve b is that obtained from the intercept of the  $Q_r$  versus  $\theta^{1/2}$  plot giving the amount of deposit formed on the electrode after the forward step. Curve c is calculated by multiplying the total charge from the reduction of  $MV^{2+}$  to  $MV^{+\bullet}$  by a factor of 2, thus, this would be the total charge passed for reduction of  $MV^{2+}$  in the absence of conproportionation. Dataset a appears to consist of two distinct regions. A sharp rise in charge occurs at low loadings (dotted line) followed by a slightly slower increase at high loadings (dashed line). For the low loading region, the concentration of  $MV^{2+}$  in solution increases as the loading increases. The increase in concentration of  $MV^{2+}$  at the electrode surface causes the rate of deposition and the rate of conproportionation to increase. A rapid increase of  $MV^{+\bullet}$  concentration at the electrode surface will result when the rate of the conproportionation reaction is large. Since the electrode is not saturated with a  $MV^\circ$  deposit,  $MV^{+\bullet}$  is reduced by the electrode to produce more  $MV^\circ$ . This reaction sequence continues and therefore amplifies the charge passed in the forward step. At high loadings of  $MV^{2+}$  the amount of  $MV^\circ$  that is deposited levels off (curve b). When the deposit is saturated, only reaction 3 accounts for the recorded charge. The further increase in charge is a result of an increase in the rate of reaction 3 due to an increase in  $MV^{2+}$  concentration. Therefore, the dashed line region of curve a is parallel to curve c.

Identification of deposition–dissolution phenomena indicate that most of the charge passed in the forward step is due to the reduction of  $MV^{2+}$  to  $MV^{+\bullet}$ . Some of the latter diffuses away from the electrode and is thus unavailable for the reoxidation in the reverse step. This conclusion is consistent with the experimental observation of a blue coloration of the electrolyte solution. However, methyl viologen cation radicals formed in

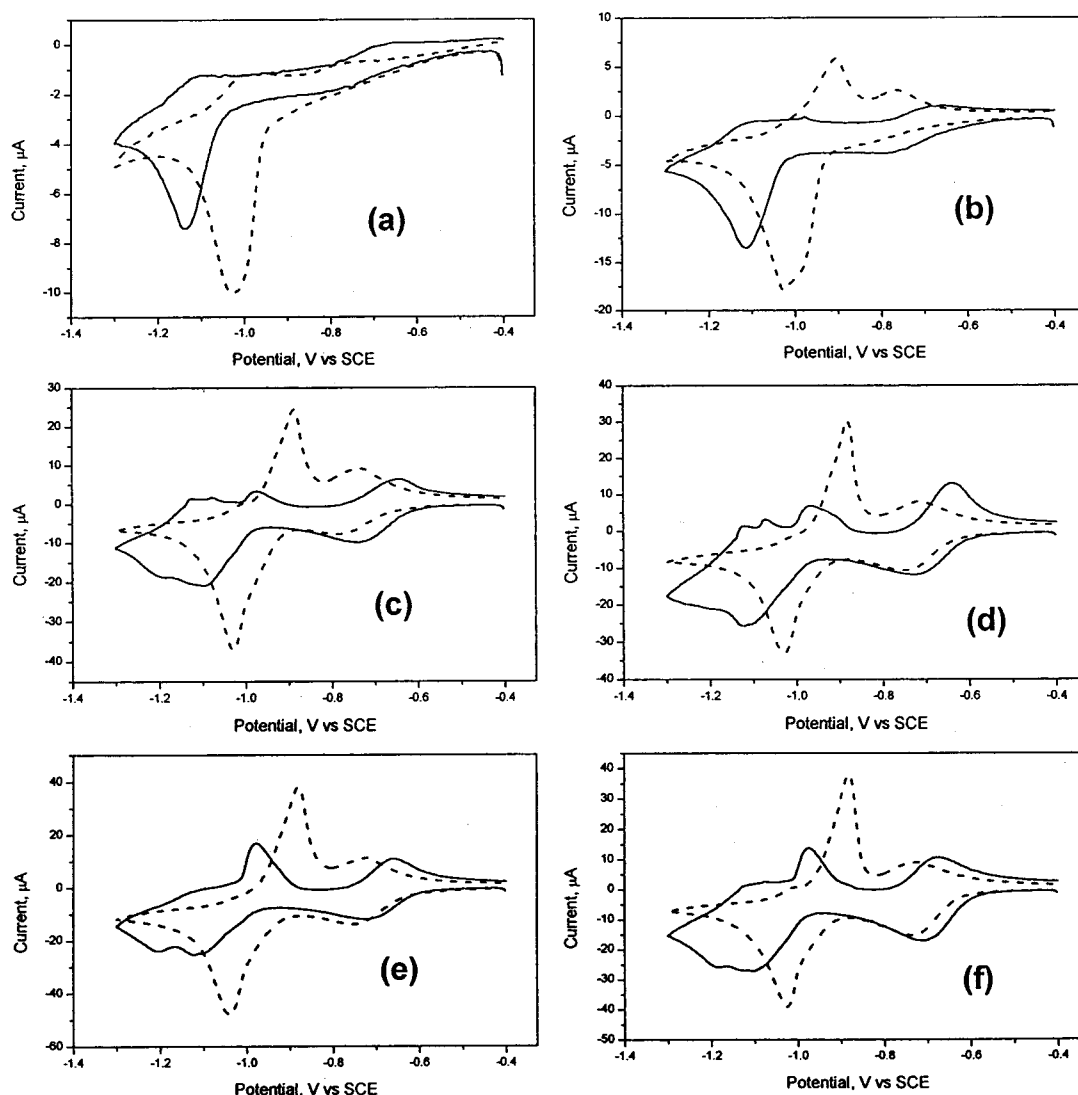


**Figure 6.** Cyclic voltammetry of (a) 3.2%, (b) 8.3%, (c) 25%, (d) 37%, (e) 42%, and (f) 58% MVY. Solid lines: 0.05 M LiCl + 50 mM LiDS. Dashed line: 0.1 M LiCl. Scan rate: 20 mV/s.

solution can ion exchange into zeolite Y. Following this, one must address the possibility that these influence the subsequent electrochemistry. Redox processes of intrazeolite cation radicals would necessitate intrazeolite electron transfer. Reduction to  $MV^0$  could then be followed by intrazeolite comproportionation. Redox of methyl viologen cation radicals is likely to occur via an extrazeolite mechanism, as we have previously discussed.<sup>1</sup> Also, the distinct behavior observed for Li- and Cs-containing electrolytes (and see later in Discussion) is important to consider. The rate of ion exchange of  $MV^{2+}$  with  $Cs^+$  is faster than with  $Li^+$ . This is due to the solvated radii of the alkali cations that are important in governing the ion exchange rate of supercage viologens. Thus more  $MV^{2+}$  will be produced by using a Cs-containing electrolyte. This will necessarily lead to more  $MV^{\bullet+}$ . If the cation radicals that reinsert into the zeolite are playing a significant role, then one would expect to see more comproportionation than with a Li-containing electrolyte. This is not the case. Both our work and that of Calzaferri et al. show that comproportionation is larger in the case of a Li-containing electrolyte. Moreover, the  $MV^0$  deposits block the electrode so that the reoxidation of  $MV^{\bullet+}$  is hindered during the reverse potential step, and as a result only the deposit is reoxidized. Together, these results suggest that deposition of  $MV^0$  on the conductive electrode surface and not in the zeolite pores is the

source of the comproportionation reaction and that intrazeolite comproportionation is insignificant.

**Anionic Surfactant Effects.**  $MV^0$  is solvated by surfactant micelles and the electrochemistry in the solution phase has been studied by Kaifer and Bard.<sup>10</sup> Figure 6 shows a distinct anionic micellar effect on the cyclic voltammetry of MVY at various loadings of  $MV^{2+}$ . At all loadings, the second reduction wave is greatly attenuated in the presence of lithium dodecyl sulfate (LiDS). The peak potential of  $MV^{\bullet+}$  reduction also shows a cathodic shift ranging from 64 to 106 mV with a 40 to 61 mV anodic shift for ( $MV^{2+}/MV^{\bullet+}$ ) depending on the loading. The shifts in peak potential are consistent with those that we observed in the solution phase<sup>13</sup> (i.e., 100 mV cathodic shift of  $E_{1/2}$  of  $MV^{\bullet+}/MV^0$  and 23 mV anodic shift in  $E_{1/2}(MV^{2+}/MV^{\bullet+})$ ). Once again, small currents in the reverse scan are due to loss of viologen from the electactive zone.<sup>1</sup>

DPSC confirms that deposition of  $MV^0$  is greatly reduced in the presence of LiDS. There is a decrease of more than 30  $\mu C$  in the y-intercept of the  $Q_t$  versus  $\theta^{1/2}$  plot as shown in Figure 7. Cyclic voltammetry and DPSC thus demonstrates the correlation between the deposition of  $MV^0$  and the enhancement of the cyclic voltammetric current. The enhanced current stems from the  $MV^0$  deposit. Since the size and charge of the anionic micelles preclude entry into the zeolite pores, they can only



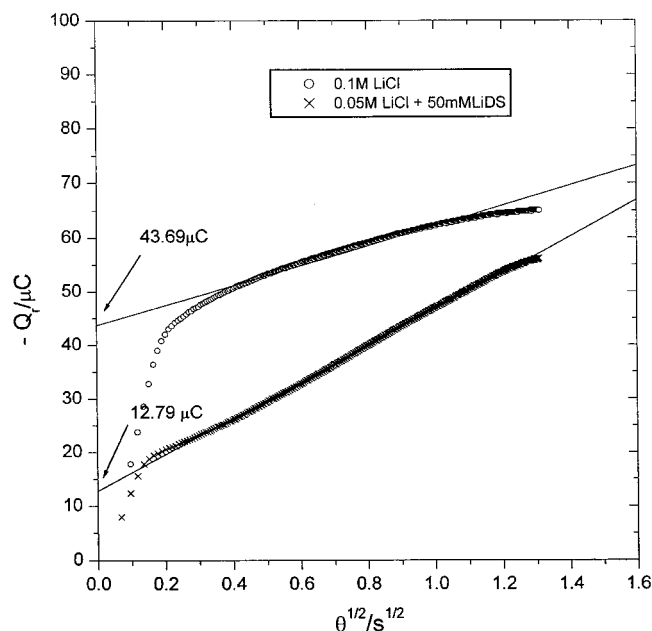


**Figure 7.**  $Q_t$  versus  $\theta^{1/2}$  plots for 8.3% MVY in 50 mM LiDS in 0.05 M LiCl ( $\times$ ) and in 0.1 M LiCl ( $\circ$ ). Potential step from  $-0.4$  to  $-1.3$  V for 5 s.

affect species outside of the zeolite particles. As a result, one can deduce that the enhanced current observed in cyclic voltammetry (see Figure 1 for example) is due to the concurrent effects of deposition and conproportionation occurring outside of the zeolite particles.

**Solution Electrochemistry vs ZMEs Electrochemistry.** Deposition and conproportionation thus occur outside of the zeolite bulk. The effect of the zeolite on the electrochemistry of  $MV^{2+}$  can, however, be understood if the concentration profiles of  $MV^{2+}$  and  $MV^\circ$  are considered. In the solution phase, and in the absence of a zeolite modifier, the diffusion layer of  $MV^{2+}$  grows during the cathodic scan with a thickness given approximately by

$$\delta(t) = 2(Dt)^{1/2} \quad (4)$$

where  $D$  is the diffusion coefficient in  $\text{cm}^2/\text{s}$ ,  $t$  is time in s, and  $\delta(t)$  is the thickness of diffusion layer at time  $t$ . The diffusion coefficient of  $MV^{2+}$  in water is  $0.86 \times 10^{-5} \text{ cm}^2/\text{s}$ .<sup>14</sup> At 20

mV/s it takes 20 s for the potential to move from the reduction potential of  $MV^{+}$  to that of  $MV^\circ$  ( $-0.9$  to  $-1.1$  V). At this time, the reduction of  $MV^{+}$  begins, and the diffusion layer is about 0.026 cm, producing essentially a zero concentration of  $MV^{2+}$  near the electrode. Conproportionation between  $MV^{2+}$  and  $MV^\circ$  is not observed. However, the presence of the zeolite at the electrode–solution interface serves as a reservoir of  $MV^{2+}$ . Thus the concentration of the dication is maintained. Concurrently, deposition of  $MV^\circ$  occurs. The presence of zeolite thus promotes conproportionation. The interesting effect of the electrolyte cation on the cyclic voltammetry of MVY originally thought to signal intrazeolite redox is also in fact a result of ion exchange rates. If we compare the behavior in Li- and Cs-containing electrolytes, then the effect is easily discerned. For LiCl, the rate of  $MV^{2+}$  exchange is slow so that loss of  $MV^{2+}$  and  $MV^{+}$  to the bulk of the solution is small on the time scale of the experiment. As a result, more  $MV^\circ$  is deposited and a larger total forward charge is observed. In CsCl, however, faster ion exchange results in depletion of viologen from the electroactive zone and a smaller forward (reductive) charge. These notions were upheld by time dependent DPSC.<sup>13</sup> For example, in the case of LiCl electrolytes, delaying the collection of data resulted in a decrease of the y-intercept and thus the amount of deposited neutral viologen. In addition, the enhanced currents in the second cathodic wave decrease as expected since they are directly controlled by the deposition of the neutral viologen.

## References and Notes

- (1) Hui, T.; Baker, M.D. *J. Phys. Chem. B* **2001**, *105*, 3204.
- (2) Walcarius, A.; Lamberts, L.; Derouane, E. G. *Electrochim. Acta* **1993**, *38*, 2267.
- (3) Gemborys, H. A.; Shaw, B. R. *J. Electroanal. Chem.* **1986**, *208*, 95.
- (4) Walcarius, A.; Lamberts, L.; Derouane, E. G. *Electrochim. Acta* **1993**, *38*, 2257.
- (5) Calzaferri, G.; Lanz, M.; Li, J. *J. Chem. Soc., Chem. Commun.* **1995**, 1313.
- (6) Engelman, E. E.; Evans, D. H. *Langmuir* **1992**, *8*, 1637.
- (7) Feng, Q.; Yue, W.; Cotton, T. M. *J. Phys. Chem.* **1990**, *94*, 2082.
- (8) Engelman, E. E.; Evans, D. H. *J. Electroanal. Chem.* **1993**, *349*, 141.
- (9) Engelman, E. E.; Evans, D. H. *J. Electroanal. Chem.* **1992**, *331*, 739.
- (10) Kaifer, A. E.; Bard, A. J. *J. Phys. Chem.* **1985**, *89*, 4876.
- (11) Anson, F. *Anal. Chem.* **1966**, *38*, 55.
- (12) Christie, J. H.; Osteryoung, R. A.; Anson, F. *J. Electroanal. Chem.* **1967**, *13*, 326.
- (13) Hui, T. MSc. Thesis University of Guelph, 1999.
- (14) Bird, C. L.; Kuhu, A. T. *Chem. Soc. Rev.* **1981**, *10*, 49.